Research Square

Preprints are preliminary reports that have not undergone peer review.
They should not be considered conclusive, used to inform clinical practice,
or referenced by the media as validated information.

Escherichia coli cell factories with altered chromosomal replication strategies exhibit accelerated growth and rapid biomass production

Hee Jin Yang
Yonsei University
Kitae Kim
Yonsei University
Soon-Kyeong Kwon
Gyeongsang National University
Jihyun F. Kim (jfk1@yonsei.ac.kr)
Yonsei University

Research Article

Keywords: replication profile, replication strategy, chromosomal landscape, cell cycle, aberrant replication origins

Posted Date: April 6th, 2022

DOI: https://doi.org/10.21203/rs.3.rs-1518101/v1

License: This work is licensed under a Creative Commons Attribution 4.0 International License.
Read Full License

Abstract

Background

Generally, bacteria have a circular genome with a single replication origin for each replicon, whereas archaea and eukaryotes can have multiple replication origins in each chromosome. In *Escherichia coli*, bidirectional DNA replication is initiated at the origin of replication (*oriC*) and arrested at the 10 termination sites (*terA–J*).

Results

We constructed *E. coli* derivatives with additional or ectopic replication origins to demonstrate the relationship between DNA replication and cell physiology. The cultures of *E. coli* derivatives with multiple replication origins contained an increased fraction of replicating cells and the cells varied in size. Without the original *oriC*, *E. coli* derivatives with double ectopic replication origins manifested impaired growth irrespective of growth conditions and enhanced cell size, and exhibited excessive and asynchronous replication initiation. The generation time of an *E. coli* strain with three replication origins decreased in a minimal medium supplemented with glucose as the sole carbon source. As well as the cell growth, the introduction of additional replication origins promoted increased biomass production.

Conclusion

Balanced cell growth and physiological stability of *E. coli* under rapid growth condition are affected by changes in the position and number of replication origins. Additionally, we show that, for the first time to our knowledge, introduction of replication initiation sites to the chromosome promotes cell growth and increases protein production.

Background

DNA replication is initiated at a specific nucleotide sequence called the origin of replication. The accuracy and speed of genome replication are essential for efficient cell division. Chromosomal DNA replication plays a major role in transferring genetic material to the next generation. Most bacteria have a circular genome with one replication initiation site, which is called *oriC*. The characteristics of archaeal replication origin are similar to those of bacterial *oriC*. However, previous studies have reported that chromosomal replication can be initiated at several loci on the chromosome [1–3]. The location of eukaryotic replication initiation is dependent on the structural properties of DNA and its topology [4, 5].

Escherichia coli has a circular chromosome with a single *oriC* and a terminus of replication (*terC*), which is located opposite to *oriC*. The order of genes on the axis defined by *oriC* and *terC* is closely related to DNA replication and the relative distance of genes from *oriC* is highly conserved in 131 γ-proteobacterial

genomes [6]. The expression of genes is influenced by their location relative to *oriC* on the *E. coli* chromosome. DNA replication can induce changes in promoter activity and copy number, which gradually decrease based on its position from *oriC* to *terC* [7]. Therefore, the unique location of *oriC* is critical for DNA synthesis and bacterial physiology.

The cell cycle of *E. coli* is generally divided into the following three periods: B period, the time between cell division and replication initiation; C period, the time required to complete DNA replication; and D period, the time required for cell division [8]. DNA replication in the cell cycle is a highly regulated process that ensures the correct and complete chromosome replication before the division of the daughter cells from the parent cells. The binding of DnaA protein, which unwinds the double-stranded DNA, initiates DNA replication at *oriC* and facilitates the recruitment of the replisome complex that is composed of replication components such as helicase, primase, and DNA polymerase III [9].

In a nutrient-rich medium, the *E. coli* cells can have a multi-forked chromosome during the exponential growth phase. Thus, the number of replication origins in rapidly dividing *E. coli* is 2^n. The *E. coli* cells can contain four or eight replication origins at one time point during rapid cell division [10]. However, a small proportion of the cells (< 5%) with ongoing DNA replication can contain atypical numbers of chromosomes (such as 3, 5, and 7) due to asynchronous replication initiation [11]. Bacterial replication pattern is dependent on cell growth conditions [12, 13]. The growth-dependent accumulation of DnaA is reported to be the primary trigger for replication initiation in *E. coli*. However, increased DnaA concentration does not affect the timing of replication initiation [10, 14]. Therefore, the balance between cell growth and DNA synthesis is maintained by the proportional increase in the copy number of chromosomes based on the growth rate.

Several studies have analyzed the roles of replication origin in chromosomal replication by inserting an additional origin or deleting the original one. The DNA replication of *E. coli* derivatives with an ectopic replication origin, which exhibited altered DNA synthesis, was correlated with transcription [15]. Another *E. coli* strain, which contains an ectopic origin *oriZ*, showed a marked variation in colony size and a delayed doubling time, which is two times higher than that of the wild type [16, 17]. Asymmetric replication partially contributes to the delayed doubling time as one replication fork progresses to replicate approximately 3.3 Mb of DNA, whereas the other fork progresses to replicate approximately 1.3 Mb of DNA [17]. In addition to bacteria, alterations in the number of replication origins influence the growth rate of an archaeon. The growth rate of *Haloferax volcanii*, which contains four replication origins, can be accelerated by removing the replication initiation sites [18].

In this study, *E. coli* strains with multiple or ectopic replication origins were constructed and their relative viability, specific growth rate, and cell volume were measured. Marker frequency and flow cytometry analyses were performed to assess the cell cycle parameters, such as the C and D periods. Replication profile analyses were performed to investigate the read counts across the whole genome and to verify the marker frequency analysis results. Moreover, an optimal culture condition for the recombinant *E. coli* strain was established to evaluate the reproducibility and repeatability of the improved growth rate of *E.*

coli derivatives. Finally, the total protein amount in the *E. coli* derivatives relative to that in the wild-type MG1655 strain was measured to determine biomass production.

Results

Construction of E. coli strains containing multiple or ectopic replication origins

The effects of the number and position of replication origins on the physiology of *E. coli* MG1655 were examined. The native replication origin region, which included both *oriC* and *mioC*, was introduced into *lacZ* (365,214–363,275 bp) or the convergent intergenic region between *dadX* and *cvrA* (1,239,951–1,250,334 bp) using the λ Red and FLP/FRT recombination systems. This modification does not directly affect bacterial cell physiology [19]. The O2 *lacZ* and O3 *lacZ dadX* strains containing two or three native replication origins, respectively, were constructed (Figs. 1B–C). To examine the activity of the newly introduced ectopic replication origins and their positional effects on the timing of replication initiation, O3 *lacZ dadX* was used as parent strains to generate strain with ectopic replication origins. The original 801-bp replication origin region, which included both *oriC* and *mioC*, of strains with multiple replication origins was replaced with the kanamycin resistance gene (*kan*). The genotypes of *E. coli* derivatives are listed in Additional file 1: Table S1. The strain with ectopic replication origins (O2' *lacZ dadX*) contained two off-site replication origins (*oriZ* and *oriZ'*) at a distance of approximately 1 Mb and 2 Mb from the location of *oriC* (Figs. 1D). Thus, the strains with two or three replication origins and two ectopic replication origins without *oriC* were constructed in this study.

Cell viability and growth phenotypes of E. coli with aberrant replication origins

The effect of replication origin (*oriC-mioC*) disruption on bacterial proliferation was examined using a bacterial cell viability assay. Flow cytometry analysis was performed to count the number of live or dead cells in a population of 2×10^4 cells. Cell viability, which was calculated as the ratio of live cells to dead cells, of the derivatives was compared with that of the wild-type MG1655 strain. The percent viabilities of O2 *lacZ* and O3 *lacZ dadX* were 97.1% and 96.8%, respectively (Additional file 1: Fig. S1A). Similarly, the percent viability of O2' *lacZ dadX* was 97.0% (Additional file 1: Fig. S1B). Thus, the strains with multiple replication origins or ectopic replication origins and the wild type exhibited similar viability. This indicated that the proliferation rates of all *E. coli* derivatives in LB were proportional to the fraction of live cells.

Next, the growth rates of wild-type MG1655 and its derivatives were determined in LB or M9 minimal medium supplemented with 0.4% glucose as the sole carbon source (Table 1). The growth rate of strains with multiple replication origins was similar to that of the wild-type strain in LB. In contrast, the growth rate of strain with ectopic replication origins was markedly lower than that of the wild-type strain in LB. The doubling time of O2' *lacZ dadX* was 39.35 ± 0.93 min, which was 60.7% longer than those of wild-type cells (24.49 ± 0.38 min). However, the growth rates of O3 *lacZ dadX* and O2 *lacZ* were 7.4% and 4.4% faster than that of MG1655 (60.79 ± 0.10 min), respectively, in M9 medium with glucose. This indicated that the growth rates were proportional to the number of replication origins when the original one is

intact. However, the growth rate of O2' *lacZ dadX* decreased by 11.8%, when compared with that of MG1655. These findings indicate that the introduction of additional replication origins can exert beneficial effects on bacterial growth under nutrient-limiting conditions. Also, the growth rate was not correlated with the number of replication origins and that the physiological changes associated with cell growth are influenced by the position and not the number of replication origin.

Table 1
Differences in cell growth of *Escherichia coli* under nutrient-rich or nutrient-limiting conditions.

Strain	LB medium			M9 medium with 0.4% glucose		
	Growth rate (h^{-1})	Generation time (min)	Difference[a] (relative ratio)	Growth rate (h^{-1})	Generation time (min)	Difference[a] (relative ratio)
MG1655	1.70 ± 0.03	24.49 ± 0.38	1.00	0.68 ± 0.01	60.79 ± 0.10	1.00
O2 *lacZ*	1.65 ± 0.02	25.26 ± 0.23	1.03	0.71 ± 0.01	58.74 ± 0.16	0.97
O3 *lacZ dadX*	1.64 ± 0.02	25.36 ± 0.28	1.04	0.73 ± 0.01	57.01 ± 0.12	0.93
O2' *lacZ dadX*	1.06 ± 0.03	39.35 ± 0.93	1.61	0.60 ± 0.01	69.08 ± 0.87	1.13

[a] The growth rates of *E. coli* strains were normalized to that of wild-type MG1655.

Data are presented as mean ± standard error.

The growth rates of the wild type and O3 *lacZ dadX* were measured under different growth conditions to determine the reproducibility of enhanced cell proliferation (Additional file 1: Table S3). LB, LB with glucose, YT, and TB, which are nutrient-rich media, were used to promote rapid growth. A minimal medium with glucose or glycerol was used for slow growth. The growth rates of O3 *lacZ dadX* were similar in different nutrient-rich media. Additionally, the growth rate of *E. coli* strains in 200 µL M9 medium with glucose in a 96-well plate was measured every 20 min using a microplate reader. Compared with those in the MG1655 cells, the growth rate increased by 15.1% and the doubling time decreased by 13.1% in O3 *lacZ dadX* cells (Additional file 1: Table S4). To confirm the growth rate of each strain in a different setting, the cells were cultured in 50 mL medium in a 250 mL Erlenmeyer flask. Again, the growth rate increased by 9.7% and the generation time decreased by 8.9% in O3 *lacZ dadX* as compared to MG1655 (Additional file 1: Table S4). The experiment was repeated three times to test the repeatability of the enhanced growth rate of O3 *lacZ dadX*. The relative growth changes in the three replicates were 9.1%, 7.3%, and 8.5% (8.3% on average; Additional file 1: Table S5). In summary, the growth rate of the strain with three replication origins was similar to that of the wild type under rapid growth conditions. However, its growth rate was faster than that of the wild type in M9 medium with glucose. Additionally, the culture volume affected the aeration during cell culture and resulted in different growth rate.

Growth-dependent morphological changes in E. coli with aberrant replication origins

Cell size was measured at the exponential or stationary phase under different growth conditions to investigate the physiological response of *E. coli* derivatives to the changes in the position and number of replication origins. The cells in the exponential phase were inoculated into fresh media and the morphology of cells was examined at the exponential phase (Additional file 1: Fig. S2). The changes in the cell volume at different growth phases of *E. coli* derivatives were examined using Gram staining. The size of the wild-type cells decreased from the exponential phase to the stationary phase in LB (Additional file 1: Table S6). The cell volume at the exponential phase was 41.7% higher than that at the stationary phase (Fig. 2A). Similarly, the size of strains with multiple replication origins decreased from the exponential phase to the stationary phase. The size of O3 *lacZ dadX* strain at the log phase decreased by 10.7% when compared with that of the wild-type strain. Additionally, the size of the O2 *lacZ* strain at the stationary phase decreased by 7.9% when compared with that of the wild-type strain. In contrast, strain with ectopic replication origins exhibited significantly decreased proliferation irrespective of growth conditions, as well as heterogeneous and increased cell size, when compared with the wild-type strain. The size of O2' *lacZ dadX* cells was 31.3% higher than that of MG1655. Meanwhile, the length of O2' *lacZ dadX* was 35.0% higher than that of MG1655.

In M9 medium with glucose, the size of wild-type and O3 *lacZ dadX* strains did not change much from the exponential phase to the stationary phase (Fig. 2B). However, the size of O2 *lacZ* and O2' *lacZ dadX* strains exhibited elongated morphology under the nutrient-deficient condition (Additional file 1: Fig. S2). At the stationary phase, the volume of O2' *lacZ dadX* strain at the exponential phase increased by 4.1%, when compared with that of the wild-type strain. Also, the cell volume of O2' *lacZ dadX* increased by 46.8%, when compared with that of the wild-type strain (Fig. 2B). These results indicated that the growth conditions markedly influenced the cell size. The cell size at the exponential phase was directly proportional to the growth rate in the nutrient-rich medium. In contrast, the cell size at the exponential phase was inversely proportional to the growth rate in the nutrient-limited medium.

Cell cycle analysis of E. coli with aberrant replication origins in LB medium

Flow cytometry analysis was performed to demonstrate the effects of additional and ectopic replication origins. *E. coli* derivatives were sampled at the early exponential phase and treated with rifampicin and cephalexin to complete in-progress replication. The left-hand peak of the DNA replication run-out histogram corresponds to the fraction of the cells with four chromosomes in which replication was not initiated. In contrast, the peak on the right corresponds to the fraction of cells with eight chromosomes, in which replication was initiated when *E. coli* derivatives were cultured in LB [10]. The DNA replication run-out histograms revealed that the culture of strains with multiple replication origins contained an increased proportion of replicating cells (Fig. 3). As a result, the fraction of replicating cells in the culture of O2 *lacZ* was similar to that in the culture of MG1655. However, the fraction of cells with eight chromosomes in the culture of O3 *lacZ dadX* was 27.5% higher than that in the culture of MG1655 (Figs. 3B–D). Compared with those in MG1655, the number of origins per cell increased by 9.3% and the

replication initiation period decreased by 32.0% in the O3 *lacZ dadX* cells (Additional file 1: Table S7). However, the duration of the C and D periods in the O3 *lacZ dadX* strain increased by 5.0% when compared with that in MG1655. In contrast, several peaks were observed in O2' *lacZ dadX*, which exhibited asynchronous and excessive replication initiation when compared with MG1655 (Fig. 3E). Hence, cell cycle parameters, such as C and D periods, the number of origins, and initiation age of O2' *lacZ dadX* was excluded. In conclusion, asymmetric replication in the strain with ectopic replication origins leads to a larger deviation on the pattern of DNA replication as compared to the wild type.

Replication profile analysis of E. coli **with aberrant replication origins**

The replication profiles of the wild type, O2 *lacZ*, and O3 *lacZ dadX* were comparatively analyzed to examine the effects of *oriZ* and *oriZ'* addition in LB (Additional file 1: Fig. S3). Genomic DNA sample was isolated from *E. coli* cells treated with sodium azide during logarithmic growth. The reference genomic DNA was prepared after treatment with rifampicin and cephalexin. The sequence reads were aligned to the reference genome and the number of sequence reads with a size of less than 1,000 bp was calculated to determine the average coverage. The replication profile analysis of MG1655 revealed bidirectional replication from *oriC* to *terC*. The average enrichment for MG1655 was the highest in the replication origin region at *oriC* and the lowest in the terminus region at *terC* (Additional file 1: Fig. S3A). In O2 *lacZ*, enrichment pattern shows the peak at the original *oriC* and *oriZ* regions (Additional file 1: Fig. S3B). Also, the genomic region of *oriZ'* in O3 *lacZ dadX* slightly increased as compared to O2 *lacZ* (Additional file 1: Fig. S3C). Generally, strains with additional replication origin shows lower enrichment near *oriC* region compared to the wild type.

In the M9 minimal medium with glucose, the replication profile of MG1655 shows sparse distribution of enrichment across the genome as compared to that in LB (Additional file 1: Fig. S3D). Also, the enrichment ratio of *ori* and *ter* was decreased. Generally, the growth rate of the cells is correlated wth the replication rate (*ori*/*ter*) of the cell [20]. Thus, the slow growth of wild-type *E. coli* in M9 medium with glucose seems associated with the reduced replication rate. In case of O3 *lacZ dadX*, distribution of the enrichment is even more sparse as compared to MG1655 (Additional file 1: Fig. S3E). However, we could observe replication initiation at the *oriZ* and *oriZ'* region in the chromosome. Although enrichment in *oriC* is similar between MG1655 and O3 *lacZ dadX*, replication initiation from the additional replication origins may contributed to accelerated growth in M9 minimal medium with glucose.

Next, we performed marker frequency analysis to measure the amount of time spent during the C and D periods in *E. coli* derivatives. The C period was calculated using the quantitative real-time polymerase chain reaction (qRT-PCR) results of the *oriC* to *terC* ratio in early exponential phase cells. The D period, which was measured as the number of origins per cell, was examined using flow cytometry analysis. The equation used to calculate the C and D periods is described in the Methods section. Twelve specific primer sets were designed to measure the variation in copy numbers of regions at every 500 kb position from *oriC* to *terC* along the right and left replichores bi-directionally. The copy number of each site in the wild-type cells gradually decreased from *oriC* to *terC* (Fig. 4). This result was consistent with that of a

previous study, which reported that the copy numbers of the left replichore were higher than those of the right replichore [21]. The *oriC* to *terC* ratio indicated that the copy numbers in the wild-type, O2 *lacZ*, and O3 *lacZ dadX* strains were 4.71 ± 0.40, 2.03 ± 0.21, and 3.10 ± 0.55, respectively, in LB. The *oriC*/ *terC* ratio in the O2 *lacZ* strain decreased by 57.0% when compared with that in the wild-type strain. The copy number in the O3 *lacZ dadX* strain recovered by 22.8% when compared with that in the O2 *lacZ* strain. In contrast, the copy number in O2' *lacZ dadX* was 3.97 ± 0.55 and 2.13 ± 0.21, respectively. For O2 *lacZ* and O2' *lacZ dadX* cells, copy numbers of the L2 region in the left replichore were higher than other regions (Fig. 4). The marker frequency analysis results revealed that the activity of the ectopic replication origins containing *oriC* and *mioC* was sufficient to initiate DNA replication and that the copy number deviation of the specific region appeared in the left replichore.

Biomass production of E. coli O3 lacZ dadX in a minimal medium

We then measured the biomass productivity using the wild type and O3 *lacZ dadX* to demonstrate the consequences of growth acceleration. The wild-type and O3 *lacZ dadX* strains exponentially growing in M9 medium with glucose as the sole carbon source were inoculated into a fresh medium. The cell growth and total protein concentration, which was used as a parameter to determine biomass, were measured every 6 h for 18 h. At each time point, the cell growth and total protein concentration varied. The biomass concentrations in O3 *lacZ dadX* at 6, 12, and 18 h were 130.02 ± 3.22, 186.46 ± 7.62, and 182.93 ± 3.28 μg mL^{-1}, respectively, whereas those in the wild type were 155.42 ± 8.16, 215.47 ± 7.62, and 227.08 ± 6.28 μg mL^{-1}, respectively (Fig. 5). The maximum biomass concentration in O3 *lacZ dadX* cells was achieved at 18 h, which was 24.1% higher than that in the wild-type strain. This indicated that biomass concentration was strongly influenced by cell growth.

Discussion

This study examined the physiological roles of the *oriC*-*terC* axis by altering the number and location of the replication origin. *oriC* is a major factor that mediates DNA synthesis and bacterial cell cycle. Hence, we hypothesized that alterations in the number or position of *oriC* can affect the usage of replication origins and consequently the efficiency of DNA replication. These alterations in the number or position of *oriC* can promote rapid growth and enable the utilization of multiple replication systems (a mechanism observed in eukaryotic DNA) in *E. coli*. The importance of the location and number of replication origins was demonstrated using three *E. coli* strains with multiple or ectopic replication origins through physiological and cell cycle analyses. The *E. coli* strains constructed in this study exhibited distinct characteristics. Although the viability of *E. coli* and its derivatives was not affected, the doubling time of the O2' *lacZ dadX* strains markedly increased irrespective of the growth conditions. This may be attributed to the asymmetric pattern in both replichores. In contrast to that in the strains with ectopic replication origins, the average growth rate of the strain with three replication origins (O3 *lacZ dadX*) increased, on average, by 8.3% in M9 minimal medium supplemented with glucose as the sole carbon source. Moreover, the biomass concentration was directly proportional to cell growth under nutrient-

limiting conditions. On the other hand, O3 *lacZ dadX* showed growth characteristics similar to the wild type in several nutrient-rich media.

To understand the role of replication initiation in cell cycle, flow cytometry and marker frequency analyses were performed to determine the time required to complete replication (C period) or cell division (D period) in LB medium. Previous studies have reported that earlier replication initiation increases the duration of the C period. Conversely, the delay in replication initiation decreases the duration of the C period [10]. The copy numbers of the left replichore were reported to be higher than those of the right replichore. Additionally, left replichore replication precedes the right replichore replication by up to 7 min [21]. Flow cytometry analysis revealed that the deviation in DNA replication and cell division in strain with ectopic replication origins was due to asynchronous DNA replication between cells with 4 and 8 chromosomes. The culture of strains with multiple replication origins exhibited an increased fraction of replicating cells.

Asymmetric replication in strain with ectopic replication origins markedly affected fork progression as the left replichore of the two replication forks from the ectopic replication origin should progress approximately twice as fast as the right fork to complete DNA replication. These results implied that the initiation of DNA replication in strain with double ectopic replication origins is compromised due to the relocation of the replication origin to an ectopic site. However, the activity of ectopic replication origins, which contain *oriC* and *mioC* genes, was sufficient to initiate DNA replication. In contrast, the specific growth rates of strains with multiple replication origins were similar. The average C + D period and the number of *oriC* per cell in the cells with multiple replication origins, which were proportional to the fraction of replicated cells, were higher than those in the wild-type strain. Marker frequency analysis revealed that the O2 *lacZ* and O3 *lacZ dadX* strains had decreased copy number at 12 loci compared to the wild type. Therefore, positional effects are considered to induce over-initiated replication, as well as to delay replication initiation.

The cell size in the log phase was larger than that in the stationary phase. The cell volumes at the stationary phase in LB were constant for *E. coli* strains with multiple replication origins, except for the O2 *lacZ* strain. The reduction in cell volume from the exponential to stationary phase was correlated with the growth rate, which declined over time in LB. However, the cell size and growth rate were not correlated in the minimal medium, which can be attributed to the limited growth rate. The introduction of ectopic replication origins and the inactivation of the native replication origin promoted heterologous changes and increased cell sizes in the cultures irrespective of growth conditions. In particular, the volume of strain with ectopic replication origins was significantly influenced by changes in genomic orientation. Consequently, the results of DNA replication run-out experiments revealed that cell size variation was dependent on the timing of replication initiation.

Although previous study showed increased cell growth after the removal of the replication origin in archaea [18], deletion of the original replication origin in *E. coli* and *Bacillus subtilis* had adverse effect on growth [22]. However, insertion of an additional replication origin to a specific site resulted in increased biomass production in M9 minimal medium with glucose, but not in nutrient-rich medium. This may be

affected by the lack of proportional increase in the production of DnaA because the activity of the replication origin is strictly regulated and limited to once per cell cycle by regulatory inactivation of DnaA (RIDA) [23]. Thus, stoichiometric analysis may be considered to define the ratio of $DnaA^{ATP}$ and $DnaA^{ADP}$ in the cells with multiple or ectopic replication origin.

The growth of cells is crucial for molecular synthesis of proteins or metabolites, because the ribosomal fraction increases as the growth rate increases, and translation process is a limiting factor for protein synthesis [24, 25]. Nevertheless, nutrients can be devoted to cell growth rather than production of target molecules. Thus, to demonstrate the production of a specific target molecule, introduction of genes related to carbon-based metabolite synthesis (e.g., 3-hydroxypropionic acid) or protein should be considered. In addition, the relocated replication origin can be attributed to head-on replication-transcription encounters that occur, because DNA polymerase and RNA polymerases share same DNA as the template. Although the overall co-directionality between replication and transcription in *E. coli* is known to be 54%, co-directionality of highly transcribed genes coding ribosomal proteins such as *rrn* C, A, B and D is 93% [26, 27]. The interference where occur in highly transcribed areas on the *E. coli* chromosome during replication and transcription can be problematic and interrupt the progression of replication forks [22, 28]. Replication-transcription interactions between replisomes are known to increase the mutation rate [29] and critical factors for balanced cell proliferation. Thus, genetic stability should be analyzed by calculating the mutation rate or tracking adaptive mutations occurring in a specific region through experimental evolution of O3 *lacZ dadX*. Further, to identify the mechanism of this growth acceleration, multi-omics analysis including transcriptome and proteome analysis could be considered.

Conclusions

This study demonstrated that the insertion of a new replication initiation site in *E. coli* can significantly influence bacterial growth, replication rate, cell cycle, and morphological features. Additionally, the insertion of an additional replication initiation site can accelerate the growth rate of *E. coli* in M9 minimal medium supplemented with glucose. This study suggested a novel mechanism to improve the growth rate and protein production in *E. coli*.

Materials And Methods

Strains and growth conditions

In this study,*E. coli*K-12 MG1655 [F^- lambda$^-$ *ilvG rfb*-50 *rph*-1 *glpK*(G184T)] was used. The *E. coli*derivatives were cultured in lysogeny broth (LB) or minimal M9 medium supplemented with 0.4% glucose as the carbon source at 37 °C with a shaking. The composition of the M9 solution was as follows: 33.9 g Na_2HPO_4, 15 g KH_2PO_4, 5 g NH_4Cl, and 2.5 g NaCl (prepared in 1 L distilled water). The following components were sterilized and added to the M9 minimal medium: 200 mL of M9 solution, 2 mL of 1 M $MgSO_4$ solution, 0.1 mL of 1 M $CaCl_2$ solution, and 20 mL of glucose (20%) (for 1 L medium). The composition of the LB medium was as follows: 10 g tryptone, 5 g yeast extract, and 5 g NaCl

(prepared in 1 L distilled water) and supplemented with antibiotics (100 μg/mL ampicillin or 50 μg/mL kanamycin). The antibiotics were used to select the *E. coli* MG1655 and its derivatives. Nutrient-rich media (LB, LB supplemented with 0.4% glucose, YT, and terrific broth (TB) medium) or minimal media (M9 medium supplemented with 0.4% glucose or 0.2% glycerol) were used to test the repeatability and reproducibility of the cell growth rate.

Selection of ectopic sites

The ectopic replication origin was introduced in the convergent intergenic region between *dadX* and *cvrA* and the coding region of *lacZ* in the *E. coli* MG1655 genome, which did not result in adverse effects on growth or physiology. Genomic properties, including the orientation of genes, location of promoters, and binding sites of transcription factors were elucidated using the EcoGene (http://www.ecogene.org/), EcoCyc (https://ecocyc.org/), and RegulonDB (http://regulondb.ccg.unam.mx/)[30-33].

Genetic manipulation of *E. coli*

oriC-mioC and *oriC* deletion cassettes were used to integrate a native replication origin into the ectopic loci and delete the original replication origin. *oriC* and *mioC* were PCR-amplified from the genomic DNA of *E. coli* MG1655. The kanamycin resistance gene with two flippase (FLP) recognition target(FRT) sequences was amplified from pKD4[19]. The *oriC-mioC* cassette comprised the replication origin of chromosome (*oriC*), the *mioC* gene, a selectable kanamycin resistance gene, two FRTsites, and two homology extension sequences (35 bp). The *oriC* deletion cassette comprised two homology extension sequences (50 bp) and a kanamycin resistance gene[15]. The insertion of *oriC-mioC* or *oriC* deletion cassette into the target regions, such as *lacZ*, intergenic region, and native replication origin was performed using λ Red recombination with the temperature-sensitive plasmid pKD46 expressing the λ Red proteins(*γ*, *β*, and *exo)* [19]. The recombinant *E. coli* cells harboring pKD46 were cultured at 30 °C. The expression of λ Red proteins was induced using 10 mM L-arabinose. The target regions were directly disrupted by transforming the *oriC-mioC* or *oriC* deletion cassettes. The recombinant *E. coli* cells were selected on L agar plates containing antibiotics and the genotype was confirmed using direct colony PCR. After the curing step of pKD46, kanamycin resistance genes of *E. coli* derivatives with multiple replication origins were eliminated using FLP/FRT recombination through the transformation of the FLP helper plasmid pCP20. The pCP20 plasmid expresses FLP recombinase that acts on the repeated FRT sites flanking the resistance gene. Next, pCP20 was eliminated by culturing the cells at 42 °C.

Growth rate analysis

For Erlenmeyer flask culture, each strain was inoculated into 3 mL of LB or M9 minimal medium supplemented with 0.4% glucose and cultured overnight at 37 °C. The optical density at 600 nm (OD_{600nm}) was measured using an OPIZEN POP spectrophotometer (Mecasys, Korea). The OD_{600nm} value of the stationary phase cultures of *E. coli* was diluted to less than 0.05 in 50 mL of fresh medium. The diluted samples were cultured to an OD_{600nm} value of less than 0.5. The amount of inoculum for determining the initial OD_{600nm} at time zero was calculated based on the OD_{600nm} value of 0.05 in 50 mL

fresh growth medium. The exponential phase cultures were then diluted in fresh growth medium and cultured to an OD_{600nm} value of 0.3 for growth rate analysis. Therefore, *E. coli*cells in the exponential phase were used to determine the growth rate. Growth curve analysis of *E. coli* MG1655 and its derivatives was performed by measuring the OD_{600nm} of triplicate cultures. The OD_{600nm} values of exponential phase *E. coli*cultures were recorded at a range of 0.05–0.3 to calculate the specific growth rate[34]. The specific growth rate (μ), whichwas defined as the linear slope in a plot of ln (OD_{600nm}) versus time (h), was calculated using the following equation:

$$\text{Specific growth rate } (\mu) = \frac{\ln(N/N_0)}{t}$$

where N or $N_0$is the optical density of *E. coli* cells in a flask at the time in the exponential phase or at time zero, respectively, and t is the cultivation time[35]. Additionally, the specific growth rates of wild-type and O3*lacZ dadX*strains from triplicate samples were verified using a plate reader (Epoch 2 microplate spectrophotometer, BioTek, USA). The following settings were employed for OD measurements: interval time, 20 min, shaking speed, 330 cpm, wavelength, 600 nm, temperature, 37 °C, temperature gradient, 1 °C, read speed, normal, read delay, 100 ms, number of measurements/data point, 8. The log phase *E. coli*culture was re-inoculated into 200μL of fresh culture medium in 96-well plates. The$OD_{600nm}$was measured using a microplate reader to determine the specific growth rates using the sameprocessesas described above.

Cell morphology analysis

The stationary or exponential phase *E. coli* cultures were harvested and subjected to Gram staining[36]. The stained *E. coli* cells were observed using a Nikon Eclipse Ci-E microscope under a 100X immersion oil lens (NA 1.45). The images were captured using NIS-Elements software. Cell length (l) and width (*w*) were analyzed using the image analysis program ImageJ with the ObjectJ plugin (Object-Image version 2.21) [37]. The length and width of 200 individual cells were measured under each growth condition. For cell volume (V) measurements, the cells were assumed to have a cylindrical structure capped by two hemispherical ends as the dividing cells only exhibited an "8" morphology. Cell volume was calculated by measuring the length and width of dividing cells using the following equation[38]:

$$\text{Cell volume } (V) = \frac{\left[\pi \times w^2 \times \left\{l - \left(\frac{w}{3}\right)\right\}\right]}{4}$$

Cell viability analysis

Cell viability was determined using the Live/Dead BacLight bacterial viability kit (Molecular Probes, L7012). The *E. coli*cells were cultivated in a 250 mL flask containing 50 mL of LB medium until the late log phase. The bacterial culture (25 mL) was centrifuged at 1,000 *g* for 15 min and the pellet was

resuspended in 2 mL of 0.85% NaCl. Next, 1 mL of *E. coli* suspension was mixed with 20 mL of 0.85% NaCl (for live cells) or 70% isopropanol (for dead cells) in 50 mL Falcon tubes and incubated for 1 h. The samples were then centrifuged at 1000 g for 15 min. The pellet was resuspended and aliquoted into separate tubes containing 10 mL of 0.85% NaCl. The OD_{600nm} was measured to determine the number of *E. coli* cells. The *E. coli*suspension was mixed in different ratios of live cells to dead cells (100:0, 50:50, and 0:100) to a volume of 3 mL and the number of cells was adjusted to 1×10^7 cells/mL (~0.01 OD_{600nm}).The *E. coli*suspension (3 mL) containing live or dead cells was incubated with 6 µL of the SYTO9 (3.34 mM) and propidium iodide (20 mM) (1:1) mixture at room temperature in the dark for more than 15 min. The number of live or dead cells was calculated using flow cytometric analysis. The SYTO9 and propidium iodide fluorescence intensities were measured at emission wavelengths of were measured at 538 and 620 nm, respectively, and an excitation wavelength of 485 nm using a flow cytometer (BD LSR II cytometer, BD Biosciences). The relative bacterial cell viability was then obtained using the following equation:

$$\text{Bacterial cell viability (\%)} = \left(\frac{\text{the number of live cells}}{\text{the number of live and dead cells}} \right) \times 100$$

Flow cytometry analysis

The number of origins per cell was determined using the replication run-out method[39]. The fresh stationary phase cultures were diluted 200-fold to an OD_{600nm} of 0.01 and cultured to an OD_{600nm} of 0.4 in LB medium. For replication run-out, the exponential phase culture was incubated with rifampin (150µg/mL, Sigma-Aldrich, USA) and cephalexin (10µg/mL, Sigma-Aldrich, USA) to prevent replication initiation and cell division for at least 3 h and chilled on ice for 5 min. All steps were performed at 4 °C. The cultures (2 mL) of the wild type or its derivatives were centrifuged at 300 g for 15 min. The pellet was washed twice with 1 mL Tris-EDTA (TE) buffer (10 mM Tris HCl (pH 7.4) and 10 mM EDTA), resuspended in 0.1 mL TE buffer, and fixed with 0.9 mL of 77% ethanol at −20 °C overnight or longer. The fixed sample was washed twice with 1 mL of TM buffer (10 mM Tris HCl (pH 7.4) and 10 mM $MgSO_4$). The OD_{600nm} of the cell suspensions was then determined. The final volume of the cell suspension (1×10^6 cells) was adjusted to 0.5–1 mL in TM buffer. Next, the cells were incubated with Hoechst 33342 (Molecular Probes, USA) solution in TM buffer (final concentration of 0.5µg/mL) for at least 30 min in the dark. Flow cytometry was performed using a flow cytometer (BD LSR II cytometer, BD Biosciences, USA). A Coherent Sapphire 488 nm laser was used to generate forward and side scatter signals, while a Lightwave Xcite 355 nm (UV) laser was used to generate fluorescence signals. Additionally, a 505 LP dichroic mirror and a 440/40 band-pass filter were used to detect Hoechst 33342 fluorescence[40]. Raw data (fcs3.0) were transformed and analyzed using FlowJo (version 10.2).

Marker frequency analysis

The copy numbers of *oriC* and specific regions from *oriC* to *terC* were determined using qRT-PCR analysis. The delta delta CT ($2^{-\Delta\Delta CT}$) method was used for relative quantification[41,42]. The *E. coli* cells for analyzing replicating genomic DNA samples were cultured to an OD_{600nm} of 0.4, treated with sodium azide (30μg/mL, Fluka BioChemika, Switzerland), and incubated for 3 h at 37 °C. Genomic DNA was extracted using the Wizard® genomic DNA purification kit (Promega) and amplified using qRT-PCR system (ABI 7300, Applied Biosystems, USA) with premix (iTaq™ Universal SYBR® Green Supermix, Bio-Rad, USA). Twelve loci that included proximal regions for both *oriC* and *terC*, as well as specific priming regions per 500 kb from the origin (*oriC*) to terminus (*terC*) along the right and left replichores were used to profile the growth-dependent differences in the copy numbers in each priming region (see Additional file 1: Table S2). Cycle threshold (Ct) obtained from wild-type *E. coli* or its derivatives was analyzed using the $2^{-\Delta\Delta Ct}$ method. Marker frequency ratios were normalized to the *oriC* to *terC* ratio of each reference genomic DNA sample from *E. coli* cells treated with rifampicin (150μg/mL, Sigma-Aldrich, USA) and cephalexin (10μg/mL, Sigma-Aldrich, USA)[10].

Replication profile analysis

The read counts across the genome of *E. coli* strains were determined using replication profile analysis. Genomic DNA from cultures of *E. coli* strains was extracted as described in the marker frequency analysis and subjected to next-generation sequencing. The genomic DNA was sequenced using Illumina HiSeq™ (50 bp or 100 bp single reads) or NovaSeq at Macrogen, Korea. The sequencing reads were imported into the CLC Genomics Workbench 9.0 (QIAGEN Bioinformatics, Germany) and assembled to the reference chromosome. The assembly was performed with the following parameters: 0.01 trim using quality scores, 15 discard reads below length, 2 mismatch cost, 3 insertion cost, 3 deletion cost, 0.5 length fraction, and 0.8 similarity fraction. Assembly data were mapped to the reference chromosome. The CSV files of the resulting mapping data were exported, and the average coverage per 1,000 bp was calculated.

Measurement of cell cycle parameters

The ratio of *oriC* to *terC* (*oriC*/*terC*) was determined using the marker frequency analysis described above. The C period was calculated using the following equation[14]:

$$\text{C period} = \frac{\ln\left(\frac{oriC}{terC}\right) \times \tau}{\ln(2)}$$

where is the generation time of each *E. coli* strain in the exponential phase. Furthermore, the chromosome number at the exponential phase was determined using flow cytometry analysis as described above. The exponential phase of *E. coli* culture in LB medium was assumed to contain a mixture of 4N cells that have not initiated DNA replication and 8N cells that have completed DNA replication. Each fraction of the DNA contents was multiplied by chromosome equivalents (4 or 8) and added to determine the *oriC* per cell. The D period was calculated using the following formula:

$$\text{D period} = \frac{\ln\left(\frac{oriC}{\text{cell}}\right) \times \tau}{\ln(2)} - \text{C period}$$

The initial age (a_i) was measured using the following equation[43]:

$$a_i = -\frac{(\ln(1-\frac{F}{2}))}{\ln(2)}, 0 \leq a_i \leq 1$$

where *F*was the fraction of *E. coli*cells that have not initiated DNA replication.

Declarations

Ethics approval and consent to participate.

Not applicable.

Consent for publication

Not applicable.

Availability of data and materials

The sequences used in this study were deposited in Sequence Read Archive (SRA) under BioProject number PRJNA722362, which comprises 20 FASTQ files for Illumina HiSeq paired-end reads of MG1655 and O3 *lacZ dadX* in LB or M9 medium with glucose treated with sodium azide or rifampicin and cephalexin, as well as those of O2 *lacZ* in LB treated with sodium azide or rifampicin and cephalexin. The nucleotide sequences of plasmids, recombination cassettes, genomic loci near recombination site were deposited in SynBioHub under collection ID ME2022KK, which comprises nine GBK files for three plasmids, three recombination cassettes, and three genomic regions. All bacterial strains in this study are available with Material Transfer Agreement.

Competing interests

The authors declare no competing interests.

Funding

This work was supported by the National Research Foundation of Korea (NRF-2016R1E1A1A01943552), and the Global Frontier Intelligent Synthetic Biology Center (NRF-2012M3A6A8053632). Publication was supported in part by the Brain Korea 21 program, and Hee Jin Yang and Kitae Kim are fellowship awardees of this program.

Authors' contribution

J.F.K conceptualized, designed, and directed the study. H.J.Y conducted most experiments and observed the phenotypes. H.J.Y., K.K, and S.K.K interpreted the results and drafted the manuscript. J.F.K, K.K., and H.J.Y reviewed and edited the manuscript. All authors discussed the results and commented on the manuscript.

Acknowledgments

We thank Yuna Jung for important insights and helpful feedback.

References

1. Norais C, Hawkins M, Hartman AL, Eisen JA, Myllykallio H, Allers T. Genetic and physical mapping of DNA replication origins in *Haloferax volcanii*. PLoS Genet. 2007; 3:e77.
2. Lundgren M, Andersson A, Chen L, Nilsson P, Bernander R. Three replication origins in *Sulfolobus* species: synchronous initiation of chromosome replication and asynchronous termination. Proc Natl Acad Sci USA. 2004; 101:7046–7051.
3. Pelve EA, Lindas AC, Knoppel A, Mira A, Bernander R. Four chromosome replication origins in the archaeon *Pyrobaculum calidifontis*. Mol Microbiol. 2012; 85:986–995.
4. Remus D, Beall EL, Botchan MR. DNA topology, not DNA sequence, is a critical determinant for *Drosophila* ORC-DNA binding. EMBO J. 2004; 23:897–907.
5. Prioleau MN, MacAlpine DM. DNA replication origins-where do we begin? Genes Dev. 2016; 30:1683–1697.
6. Sobetzko P, Travers A, Muskhelishvili G. Gene order and chromosome dynamics coordinate spatiotemporal gene expression during the bacterial growth cycle. Proc Natl Acad Sci USA. 2012; 109:E42-50.
7. Bryant JA, Sellars LE, Busby SJ, Lee DJ. Chromosome position effects on gene expression in *Escherichia coli* K-12. Nucleic Acids Res. 2014; 42:11383–11392.
8. Wang JD, Levin PA. Metabolism, cell growth and the bacterial cell cycle. Nat Rev Microbiol. 2009; 7:822–827.
9. Mott ML, Berger JM. DNA replication initiation: mechanisms and regulation in bacteria. Nat Rev Microbiol. 2007; 5:343–354.
10. Hill NS, Kadoya R, Chattoraj DK, Levin PA. Cell size and the initiation of DNA replication in bacteria. PLoS Genet. 2012; 8:e1002549.
11. Skarstad K, Boye E, Steen HB. Timing of initiation of chromosome replication in individual *Escherichia coli* cells. EMBO J. 1986; 5:1711–1717.
12. Akerlund T, Nordstrom K, Bernander R. Analysis of cell size and DNA content in exponentially growing and stationary-phase batch cultures of *Escherichia coli*. J Bacteriol. 1995; 177:6791–6797.

13. Stokke C, Flatten I, Skarstad K. An easy-to-use simulation program demonstrates variations in bacterial cell cycle parameters depending on medium and temperature. PLoS One. 2012; 7:e30981.
14. Flatten I, Fossum-Raunehaug S, Taipale R, Martinsen S, Skarstad K. The DnaA protein is not the limiting factor for initiation of replication in *Escherichia coli*. PLoS Genet. 2015; 11:e1005276.
15. Rudolph CJ, Upton AL, Stockum A, Nieduszynski CA, Lloyd RG. Avoiding chromosome pathology when replication forks collide. Nature. 2013; 500:608–611.
16. Dimude JU, Stein M, Andrzejewska EE, Khalifa MS, Gajdosova A, Retkute R, Skovgaard O, Rudolph CJ. Origins Left, Right, and Centre: Increasing the Number of Initiation Sites in the *Escherichia coli* Chromosome. Genes. (Basel) 2018; 9.
17. Ivanova D, Taylor T, Smith SL, Dimude JU, Upton AL, Mehrjouy MM, Skovgaard O, Sherratt DJ, Retkute R, Rudolph CJ. Shaping the landscape of the *Escherichia coli* chromosome: replication-transcription encounters in cells with an ectopic replication origin. Nucleic Acids Res. 2015; 43:7865–7877.
18. Hawkins M, Malla S, Blythe MJ, Nieduszynski CA, Allers T. Accelerated growth in the absence of DNA replication origins. Nature. 2013; 503:544–547.
19. Datsenko KA, Wanner BL. One-step inactivation of chromosomal genes in *Escherichia coli* K-12 using PCR products. Proc Natl Acad Sci USA. 2000; 97:6640–6645.
20. Korem T, Zeevi D, Suez J, Weinberger A, Avnit-Sagi T, Pompan-Lotan M, Matot E, Jona G, Harmelin A, Cohen N, et al. Growth dynamics of gut microbiota in health and disease inferred from single metagenomic samples. Science. 2015; 349:1101–1106.
21. Joshi MC, Bourniquel A, Fisher J, Ho BT, Magnan D, Kleckner N, Bates D. *Escherichia coli* sister chromosome separation includes an abrupt global transition with concomitant release of late-splitting intersister snaps. Proc Natl Acad Sci USA. 2011; 108:2765–2770.
22. Srivatsan A, Tehranchi A, MacAlpine DM, Wang JD. Co-orientation of replication and transcription preserves genome integrity. PLoS Genet. 2010; 6:e1000810.
23. Skarstad K, Katayama T. Regulating DNA replication in bacteria. Cold Spring Harb Perspect Biol. 2013; 5:a012922.
24. Sanden AM, Prytz I, Tubulekas I, Forberg C, Le H, Hektor A, Neubauer P, Pragai Z, Harwood C, Ward A, et al. Limiting factors in *Escherichia coli* fed-batch production of recombinant proteins. Biotechnol Bioeng. 2003; 81:158–166.
25. Metzl-Raz E, Kafri M, Yaakov G, Soifer I, Gurvich Y, Barkai N. Principles of cellular resource allocation revealed by condition-dependent proteome profiling. Elife. 2017; 6.
26. Brewer BJ. When polymerases collide: replication and the transcriptional organization of the *E. coli* chromosome. Cell. 1988; 53:679–686.
27. McLean MJ, Wolfe KH, Devine KM. Base composition skews, replication orientation, and gene orientation in 12 prokaryote genomes. J Mol Evol. 1998; 47:691–696.

28. De Septenville AL, Duigou S, Boubakri H, Michel B. Replication fork reversal after replication-transcription collision. PLoS Genet. 2012; 8:e1002622.
29. Mirkin EV, Mirkin SM. Mechanisms of transcription-replication collisions in bacteria. Mol Cell Biol. 2005; 25:888–895.
30. Rudd KE. EcoGene: a genome sequence database for *Escherichia coli* K-12. Nucleic Acids Res. 2000; 28:60–64.
31. Zhou J, Rudd KE. EcoGene 3.0. Nucleic Acids Res. 2013; 41:D613-624.
32. Karp PD, Weaver D, Paley S, Fulcher C, Kubo A, Kothari A, Krummenacker M, Subhraveti P, Weerasinghe D, Gama-Castro S, et al. The EcoCyc Database. EcoSal Plus. 2014; 6.
33. Gama-Castro S, Jimenez-Jacinto V, Peralta-Gil M, Santos-Zavaleta A, Penaloza-Spinola MI, Contreras-Moreira B, Segura-Salazar J, Muniz-Rascado L, Martinez-Flores I, Salgado H, et al. RegulonDB (version 6.0): gene regulation model of Escherichia coli K-12 beyond transcription, active (experimental) annotated promoters and Textpresso navigation. Nucleic Acids Res. 2008; 36:D120-124.
34. Sezonov G, Joseleau-Petit D, D'Ari R. *Escherichia coli* physiology in Luria-Bertani broth. J Bacteriol. 2007; 189:8746–8749.
35. Lee DH, Feist AM, Barrett CL, Palsson BO. Cumulative number of cell divisions as a meaningful timescale for adaptive laboratory evolution of *Escherichia coli*. PLoS One. 2011; 6:e26172.
36. Bartholomew JW, Mittwer T. The Gram stain. Bacteriol Rev. 1952; 16:1–29.
37. Vischer NO, Verheul J, Postma M, van den Berg van Saparoea B, Galli E, Natale P, Gerdes K, Luirink J, Vollmer W, Vicente M, den Blaauwen T. Cell age dependent concentration of *Escherichia coli* divisome proteins analyzed with ImageJ and ObjectJ. Front Microbiol. 2015; 6:586.
38. Volkmer B, Heinemann M. Condition-dependent cell volume and concentration of *Escherichia coli* to facilitate data conversion for systems biology modeling. PLoS One. 2011; 6:e23126.
39. Skarstad K, Bernander R, Boye E. Analysis of DNA replication *in vivo* by flow cytometry. Methods Enzymol. 1995; 262:604–613.
40. Kim MS, Bae SH, Yun SH, Lee HJ, Ji SC, Lee JH, Srivastava P, Lee SH, Chae H, Lee Y, et al. Cnu, a novel *oriC*-binding protein of *Escherichia coli*. J Bacteriol. 2005; 187:6998–7008.
41. Pfaffl MW. A new mathematical model for relative quantification in real-time RT-PCR. Nucleic Acids Res. 2001; 29:e45.
42. Rao X, Huang X, Zhou Z, Lin X. An improvement of the 2^(-delta delta CT) method for quantitative real-time polymerase chain reaction data analysis. Biostat Bioinforma Biomath. 2013; 3:71–85.
43. Wold S, Skarstad K, Steen HB, Stokke T, Boye E. The initiation mass for DNA replication in *Escherichia coli* K-12 is dependent on growth rate. EMBO J. 1994; 13:2097–2102.

Figures

Figure 1

***Escherichia coli* derivatives with multiple or ectopic replication origins.** The circles represent the chromosome of the *E. coli* MG1655 (4.6 Mb) and its derivatives. The gray triangle indicates the replication termination sites on the chromosome. (A) Wild-type MG1655. (B) O2 *lacZ* with two replication origins. (C) O3 *lacZ dadX* with three replication origins. (D) O2' *lacZ dadX* with two ectopic replication origins.

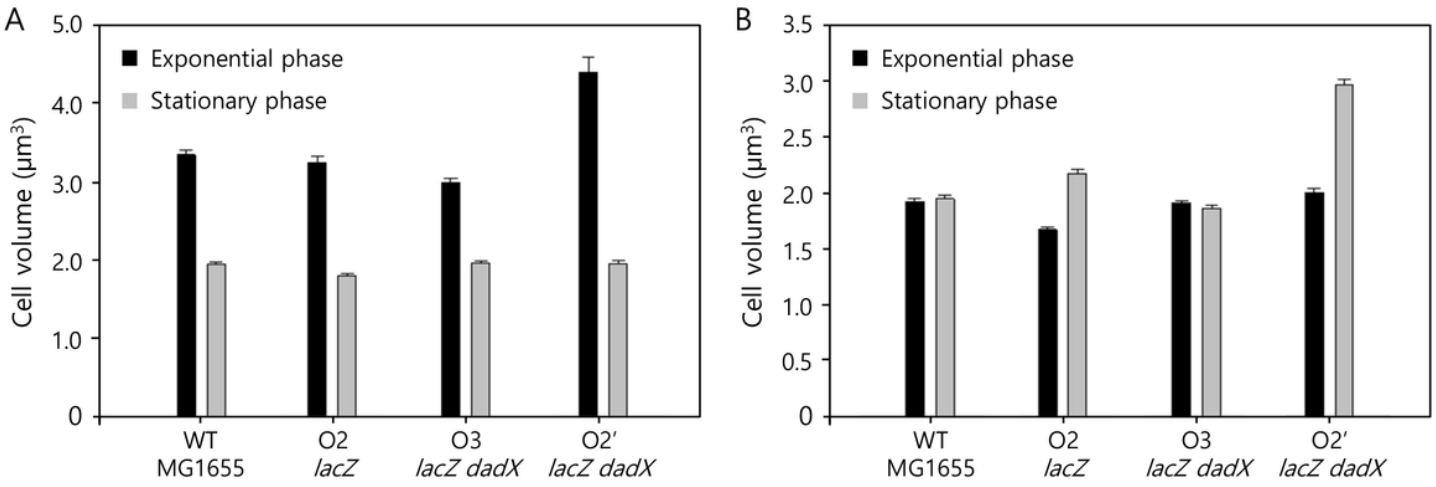

Figure 2

Cell size variation of *Escherichia coli* strains in different growth phases. Black or gray bars with standard errors indicated the cell volumes of the *E. coli* strains at exponential or stationary phase, respectively, in (A) Lysogeny broth or (B) M9 medium supplemented with 0.4% glucose.

Figure 3

DNA replication run-out histograms of *Escherichia coli* derivatives in lysogeny broth. Chromosome contents of each *E. coli* strain at the stationary phase (A) and exponential phase in LB medium (B–E) were determined using flow cytometry analysis. Two major peaks of Hoechst fluorescence indicated that *E. coli* cells contained four or eight chromosomes (B–D). Four to five major peaks with indistinguishable minor peaks of Hoechst fluorescence indicated that *E. coli* cells contained several copies of the chromosomes (E). (A) Wild-type cells in the stationary phase. (B) Wild-type cells in the exponential phase. (C) O2 *lacZ* cells in the exponential phase. (D) O3 *lacZ dadX* cells in the exponential phase. (E) O2' *lacZ dadX* cells in the exponential phase.

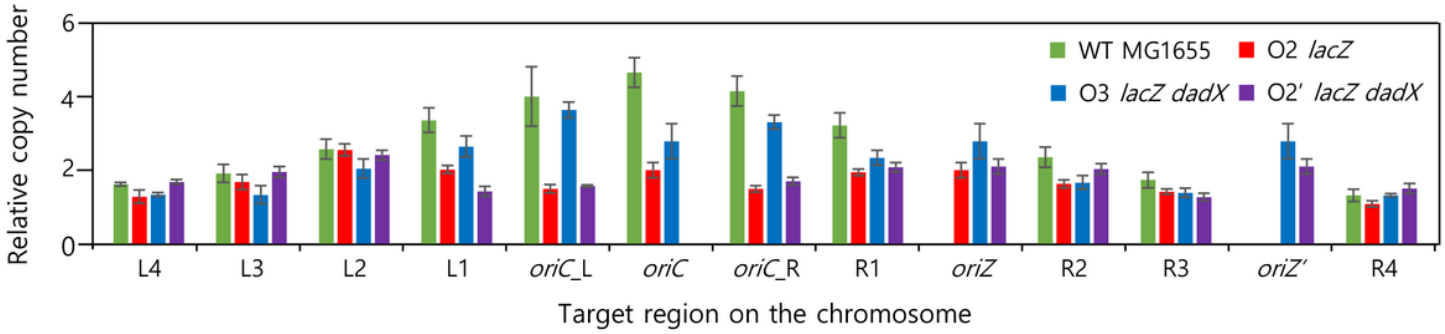

Figure 4

Chromosomal copy numbers of each locus for exponential cell populations in LB medium. The quantitative real-time PCR analysis was performed to measure the location-dependent copy number variation in the target regions of strains with multiple or ectopic replication origins. Data are presented as mean ± standard error. Both *oriZ* and *oriZ'* target regions represent the positions located near the newly introduced ectopic sites, *lacZ* and intergenic region between *dadX* and *cvrA*. Green, red, and blue, and purple bars indicate the wild type, O2 *lacZ*, and O3 *lacZ dadX*, and O2' *lacZ dadX*, respectively.

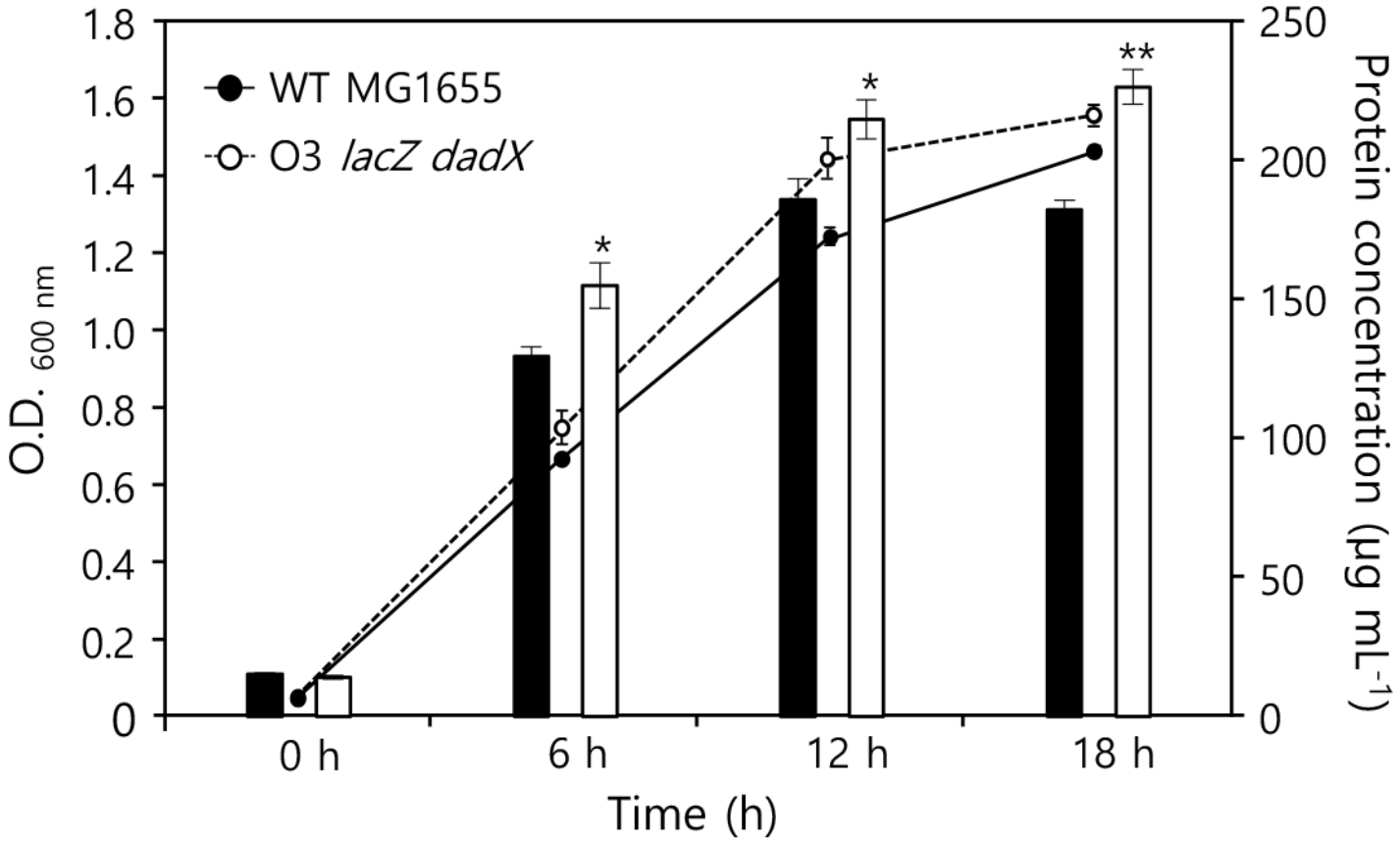

Figure 5

Growth-dependent increase of the biomass of *E. coli* O3 *lacZ dadX*. Total proteins were extracted and each optical density for Bradford assay was measured by every 6 hours for each *E. coli* strain. Black and white bars with standard errors indicated as the total protein concentration for the wild type and O3 *lacZ dadX*, respectively. A single or double asterisk indicates *p*-value either under 0.05 or 0.01.

Supplementary Files

This is a list of supplementary files associated with this preprint. Click to download.

- Additionalfile1.pdf